Comparison of two alternative sequences for human in-vivo brain MR Current Density Imaging (MRCDI)

Göksu, Cihan; Hanson, Lars G. ; Siebner, Hartwig; Ehses, Philipp; Scheffler, Klaus; Thielscher, Axel

Publication date:
2018

Document Version
Publisher's PDF, also known as Version of record

5607

Comparison of two alternative sequences for human in-vivo brain MR Current Density Imaging (MRCDI)

Cihan Göksu[1,2], Lars G. Hanson[1,2], Hartwig R. Siebner[2,3], Philipp Ehses[4,5], Klaus Scheffler[4,6], and Axel Thielscher[1,2]

[1]Center for Magnetic Resonance, DTU Elektro, Technical University of Denmark, Kgs. Lyngby, Denmark, [2]Danish Research Centre for Magnetic Resonance, Centre for Functional and Diagnostic Imaging and Research, Copenhagen University Hospital, Hvidovre, Denmark, [3]Department of Neurology, Copenhagen University Hospital, Bispebjerg, Denmark, [4]High-Field Magnetic Resonance Center, Max-Planck-Institute for Biological Cybernetics, Tübingen, Germany, [5]German Center for Neurodegenerative Diseases (DZNE), Bonn, Germany, [6]Department of Biomedical Magnetic Resonance, University of Tübingen, Tübingen, Germany

Synopsis

MRCDI is a novel technique, utilizing different phase-sensitive MR methods for non-invasive measurements of weak currents in the human body, which is important in several neuroscience applications. Here, we compare the in-vivo performance of two different MR methods, multi-echo spin echo (MESE) and steady-state free precession free induction decay (SSFP-FID), with single- vs. multi-gradient-echo readouts. We demonstrate that multi-gradient-echo readouts improve both methods. We validate the linear dependence of the measured current-induced magnetic field on the injected current strength for both methods, and propose the more efficient SSFP-FID method as being well suited for highly sensitive single-slice human in-vivo MRCDI.

Introduction

Accurate measurements of the current flow distributions, caused by neural or external sources, in the human brain in-vivo is important in several neuroscience applications. MRCDI is an emerging technique, which combines MR methods with alternating currents for in-vivo current flow measurements in the human brain at high resolution (1). The efficiency of the technique depends on the used MR method. MESE is a technique robust to field inhomogeneities and provides high signal-to-noise-ratio (SNR). On the other hand, SSFP-FID is more sensitive to current-induced phase, but more vulnerable to field inhomogeneities. Both methods are promising for in-vivo human brain MRCDI. We previously performed a thorough sensitivity comparison of MESE and SSFP-FID MRCDI in phantoms (2). However, in-vivo robustness of the methods to physiological noise was not analyzed. Here we compare MESE and SSFP-FID in-vivo, and propose SSFP-FID as a better alternative for single-slice human in-vivo brain MRCDI applications.

Methods

In MRCDI, weak alternating tissue currents, which are synchronized with an MR sequence, create a magnetic field component of the current-induced magnetic field ΔBz,c parallel to the scanner field. This causes small shifts in the precession frequency of the magnetization. These modulate the phase of the MR signal, proportional to $\Delta B_{z,c}$, and allows measurement of $\Delta B_{z,c}$ and calculations of the current flow distribution. Here, we employed MESE (Fig.1a) and SSFP-FID (Fig.1b) and used previously optimized sequence parameters (2) for human in-vivo MRCDI. First, we validated both methods by checking the linear dependence of the measured $\Delta B_{z,c}$ on the current strength I_c. A cable was wrapped around a spherical phantom (16 cm in diameter) with similar relaxation parameters as brain tissue. Using both methods, $\Delta B_{z,c}$ was measured for I_c = [0, 0.33, 0.66, 1] mA. The MESE measurements were performed with image matrix 112x90, voxel size 2x2x3mm^3, number of spin-echo N_{SE}=3, gradient-echo N_{GE}=5, bandwidth BW=103.6 Hz/pixel, echo spacing T_{ES}=60 ms, and repetition time T_R=1.5 s. The measurement was repeated N_{meas}=2 times. The SSFP-FID measurements were performed with image matrix 112x90, voxel size 2x2x3mm^3, tip angle α=30˚, N_{GE}=7, BW=75 Hz/pix, T_R=120 ms, and N_{meas}=12. The total scan times were close to ~9mins and ~4.5 mins for MESE and SSFP-FID, respectively. The same experiments were also repeated in-vivo in three participants. The average $\Delta B_{z,c}$ values were extracted, and a linear regression model fitted to the measurements. As a last step, single- and multi-gradient-echo readout performances of the methods were tested in three subjects. MESE (N_{GE}=1/5, BW = 19.2/103.6 Hz/pixel) and SSFP-FID (N_{GE}=1/7, BW = 12/75 Hz/pixel) experiments were repeated with I_c= 1 mA and without current injection. Gaussian distributions were fitted to the $\Delta B_{z,c}$ distributions of the control experiments without I_c and the methods were compared in terms of the mean shifts and the standard deviations. In the experiments, the current waveform was generated using an arbitrary waveform generator (33500B, KEYSIGHT Technologies, California, United States), amplified via an MR-conditional transcranial brain stimulator (DC-STIMULATOR PLUS, neuroConn GmbH, Germany), and injected via rubber electrodes attached to the scalp (close to the temporo-parietal junction).

Results and Discussion

The $\Delta B_{z,c}$ measurements for MESE and SSFP-FID show a linear dependence on the injected current strength in both the phantom (Fig. 2) and in-vivo (Fig. 3). The intercepts β_0 are close to zero, and the estimated slopes β_1 found similar in both methods (Fig. 4a). The results of linear regression analyses are highly significant. The use of multi-gradient-echo readouts improve the quality of the measured $\Delta B_{z,c}$ images with and without I_c. The ghosting-like artifacts disappear (Fig. 5). The results without current injection show that the mean shifts are close to zero and the standard deviations are effectively reduced by means of multi-gradient-echo readouts (Fig. 4b). MESE exhibits a lower noise floor compared to SSFP-FID in two out of three subjects. Both MESE (total scan time T_{tot}~9 mins) and SSFP-FID (T_{tot}~4.5 mins) have similarly low noise floors with standard deviations of on average ~0.1 nT.

Conclusion

Both MESE and SSFP-FID methods are validated in phantom and in-vivo experiments. The use of multi-gradient-echo readout provides better results, as systematic averaging of multi-echoes reduces detrimental effects (e.g. blood flow and motion). Both methods provide sufficiently low noise floors for human brain MRCDI. The higher number of measurements used in SSFP-FID may allow a better removal of physiological noise and outliers in the future, which may make the method the better choice for single-slice in-vivo MRCDI. However, MESE can still outperform SSFP-FID in multi-slice MRCDI, as it allows acquiring few slices without losing sensitivity (2).

Acknowledgements

The project is supported by Lundbeck foundation with grant number R118-A11308.

References

1. Scott GC, Joy MLG, Armstrong RL, Henkelman RM. Sensitivity of magnetic-resonance current-density imaging. J. Magn. Reson. 1992;97:235–254.

2. Göksu C, Scheffler K, Ehses P, Hanson LG, Thielscher A. Sensitivity Analysis of Magnetic Field Measurements for Magnetic Resonance Electrical Impedance Tomography (MREIT). Magn. Reson. Med. 2017. doi: 10.1002/mrm.26727.

Figures

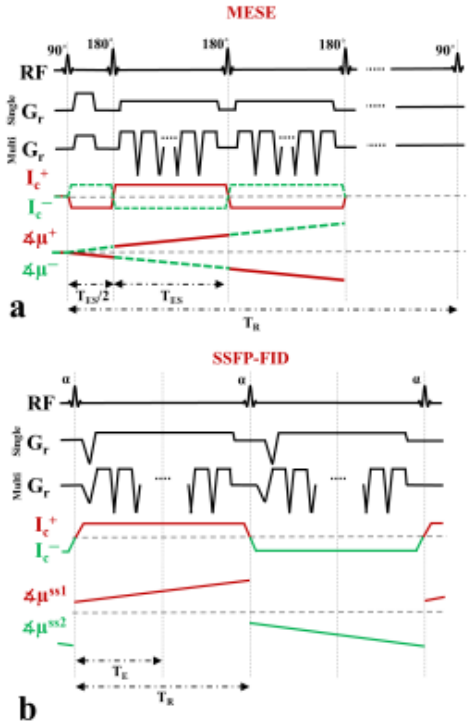

Figure 1. Schematic diagram of the (a) MESE and (b) SSFP-FID sequence (see (2) for sequence details). μ is the phase of the transverse magnetization. The currents I_c are employed in two opposite directions (indicated by green and red lines) to acquire two phase images with opposite current-induced phases. Either single-gradient-echo (single Gr, N_{GE} = 1) or multi-gradient-echo readouts (multi Gr, N_{GE} = 5 for MESE and N_{GE} = 7 for SSFP-FID) are used. The $\Delta B_{z,c}$ images are calculated from each of the single echoes, and systematically combined (2).

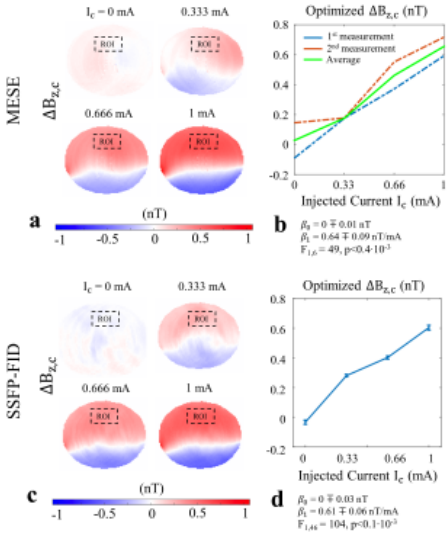

Figure 2. Testing linear dependence of the measured $\Delta B_{z,c}$ on the applied current strength I_c in the spherical phantom, performed for both MESE and SSFP-FID with multi-gradient-echo readouts. MESE results: (a) $\Delta B_{z,c}$ images. (b) Dependency plot. The results of the two measurements are shown as blue and orange dashed lines, and their average is shown as a green line. SSFP-FID results: (c) $\Delta B_{z,c}$ images. (d) Dependency plot. The average of the 12 measurements is shown; the bars represent the standard error. For both methods, the average $\Delta B_{z,c}$ was calculated in the region-of-interest (ROI) indicated by black dashed rectangles.

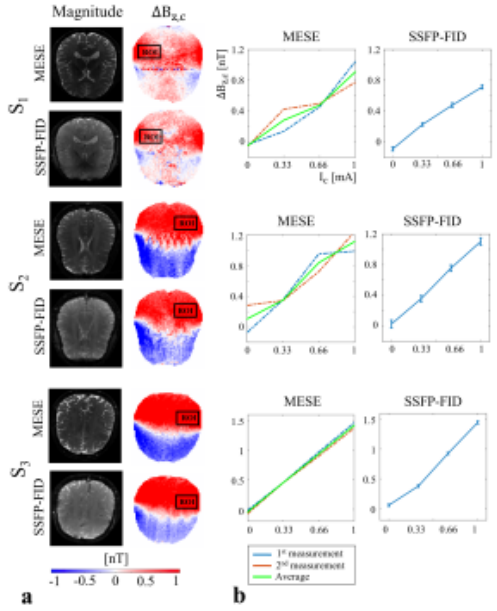

Figure 3. Testing linear dependence of the measured $\Delta B_{z,c}$ on the applied current strength I_c in three subjects, performed for both methods with multi-gradient-echo readouts. MESE results: (a) The magnitude and $\Delta B_{z,c}$ images for I_c = 1 mA. (b) Dependency plot. The results of the two measurements are shown as blue and orange dashed lines, and their average is shown as a green line. SSFP-FID results: (c) $\Delta B_{z,c}$ images. (d) Dependency plot. The average of the 12 measurements is shown; the bars represent the standard error. For both methods, the average $\Delta B_{z,c}$ was calculated in the region-of-interests (ROIs) indicated by black rectangles.

a

	MESE			SSFP-FID		
	$F_{1,6}$(p)	β_0 in [nT]	β_1 in [nT/mA]	$F_{1,46}$(p)	β_0 in [nT]	β_1 in [nT/mA]
S_1	57 ($<0.3\cdot10^{-3}$)	-0.05 (0.08)	0.90 (0.12)	46 ($<10^{-6}$)	-0.07 (0.07)	0.80 (0.12)
S_2	50 ($<0.4\cdot10^{-3}$)	0.07 (0.09)	1.03 (0.15)	27 ($<10^{-5}$)	0.02 (0.13)	1.09 (0.21)
S_3	1527 ($<10^{-6}$)	-0.04 (0.02)	1.44 (0.04)	225 ($<10^{-6}$)	-0.01 (0.06)	1.42 (0.10)

b

	MESE		SSFP-FID	
	N_{GE}=1 $\mu_{\Delta Bz,c}$ ($\sigma_{\Delta Bz,c}$)	N_{GE}=5	N_{GE}=1	N_{GE}=7
S_1	0.066 (0.166)	0.037 (0.086)	-0.043 (0.149)	0.026 (0.123)
S_2	0.126 (0.186)	0.089 (0.117)	-0.024 (0.201)	-0.012 (0.111)
S_3	0.144 (0.150)	-0.035 (0.103)	-0.078 (0.150)	-0.041 (0.151)
Avg	**0.112 (0.167)**	**0.030 (0.102)**	**-0.048 (0.167)**	**-0.009 (0.128)**

Figure 4. (a) Linear fits of the measured dependence of $\Delta B_{z,c}$ on the applied current strength. The table lists the F- and p-values, the intercepts β_0 and the slopes β_1 of the fitted linear regression models. The standard errors of β_0 and β_1 are given in brackets. (b) Comparison of single- vs. multi-gradient-echo acquisition for the case without current injection in three subjects. The table lists the mean shifts and standard deviations (given in brackets) of the noise distributions of $\Delta B_{z,c}$ values in the brain in units of nT.

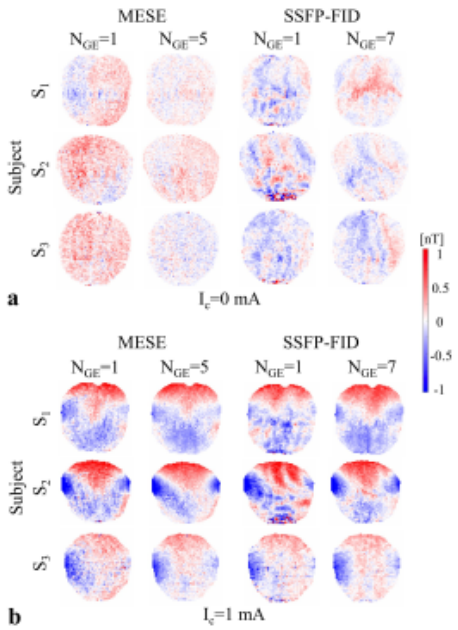

Figure 5. Comparison of single- vs. multi-gradient-echo acquisition in three subjects for both MESE (total scan time $T_{tot} \approx 9$ mins) and SSFP-FID ($T_{tot} \approx 4.5$ mins). (a) $\Delta B_{z,c}$ images of the measurements without current injection. (b) $\Delta B_{z,c}$ images of the measurements with current injection $I_c = 1$ mA. For better visualization of the spatial patterns, mean-corrected images are shown (i.e., the average $\Delta B_{z,c}$ in the brain was subtracted). Ghosting-like patterns are observed in the results of the single-gradient-echo acquisitions due to the low-bandwidth acquisition, which are eliminated in the results with multi-gradient-echo readouts.